NMR and X-ray Crystallographic Analysis of Thermodynamically Stable Tetraphenylporphyrin-Stoppered Rotaxanes

Taichi Ikeda,[a,b] Masumi Asakawa,[b] Midori Goto,[b] Yoshinobu Nagawa,[b] and Toshimi Shimizu*[b]

Keywords: Crown compounds / Porphyrinoids / Rhodium / Rotaxanes / Self-assembly

Tetraphenylporphyrin-stoppered rotaxanes, in which tetraphenylporphyrin rhodium(III) chloride serves for end-capping of the thread molecule through axial coordination, were prepared from the inclusion complexes formed between crown ether and secondary ammonium cation derivatives. Two types of the thread molecules, with different molecular lengths, were used for the rotaxane preparation. The obtained porphyrin-stoppered rotaxanes proved to be thermodynamically stable in their pure forms at room temperature. ^{1}H NMR measurements indicated that the protons of the thread molecule and the crown ether are considerably affected by the shielding effect of the terminal porphyrin. We confirmed that the intensity of the shielding effect is applicable as a probe for estimation of the location of the crown ether. We found different chemical shifts for individual members of pairs of methylene protons on the same crown ether carbon when the relatively shorter thread molecule was used, whereas we observed similar chemical shifts for those in the rotaxane with longer thread molecule. This result indicates that the stronger shielding effect of the porphyrin exposes the two faces of the crown ether to different magnetic environments in the case of the relatively shorter thread molecule. X-ray crystallography for the porphyrin-stoppered rotaxane with the relatively shorter thread molecule revealed that the crown ether forms many hydrogen bonds with the thread molecule. We confirmed that not only the hydrogen atoms of the secondary ammonium ion and the neighboring methylene groups, but also the β-hydrogen atoms of the axially coordinated pyridine moiety participate in hydrogen bond formation with the crown ether oxygen atoms. It is likely that the catechol rings of the crown ether interact with the phenyl groups of the terminal porphyrin.

Introduction

Since the first report on the synthesis and the cation-binding properties of crown ethers,[1] molecular recognition by crown ether derivatives has attracted much attention in terms of the structures and the stabilities of various kinds of complexes.[2] In particular, dibenzo[24]crown-8 (crown ether **3**, Figure 1) has been of great interest as a host molecule for dialkylammonium cation derivatives. A stable inclusion complex of crown ether **3** with dibenzylammonium derivatives has served as a useful template for the preparation of interlocked molecules such as rotaxanes in nonpolar solvents.[3] In a rotaxane molecule, the macrocycle does not covalently link to the thread molecule, but is topologically entrapped by the thread molecule with its bulky end groups. The macrocycle can thus slide and rotate on the thread molecule. This intriguing mechanical motion of the interlocked molecule has allowed us to address the fabrication of molecular devices such as motors or switches.[4]

Rotaxanes end-capped by axial coordination to metalloporphyrins have recently been reported,[5] but were not thermodynamically stable at room temperature. In our previous study, we demonstrated the preparation of a porphyrin-stoppered rotaxane in which the thread molecule of the rotaxane was axially coordinated to [5,10,15,20-tetrakis(3,5-di-*tert*-butylphenyl)porphyrin]rhodium(III) chloride.[6] The coordination bond between the pyridine moiety in the thread molecule and the rhodium porphyrin proved to be strong enough for the pure rotaxane to be obtained by conventional column chromatography at room temperature. The rotaxane preparation process, including both inclusion complexation and end-capping, requires no organic chemical reactions (Figure 2). Just mixing of the solutions under ambient condition afforded the crude rotaxane within a few minutes. The pure product is obtainable within a few hours in a high yield (70−80%), enabling us to analyze the well defined molecular structures of these porphyrin-stoppered rotaxanes. The shielding effect of the terminal porphyrin affects the chemical shifts in the NMR spectrum,[7] this fea-

[a] New Energy and Industrial Technology Development Organization,
Sunshine 60, 3-1-1 Higashiikebukuro, Toshima, Tokyo, 170-6028, Japan
[b] Nanoarchitectonics Research Center, National Institute of Advanced Industrial Science and Technology,
Tsukuba Central 5, 1-1-1 Higashi, Tsukuba, Ibaraki 305-8565, Japan
Fax: (internat.) +81-298-(0)61-4545
E-mail: tshmz-shimizu@aist.go.jp

  DOI: 10.1002/ejoc.200300289

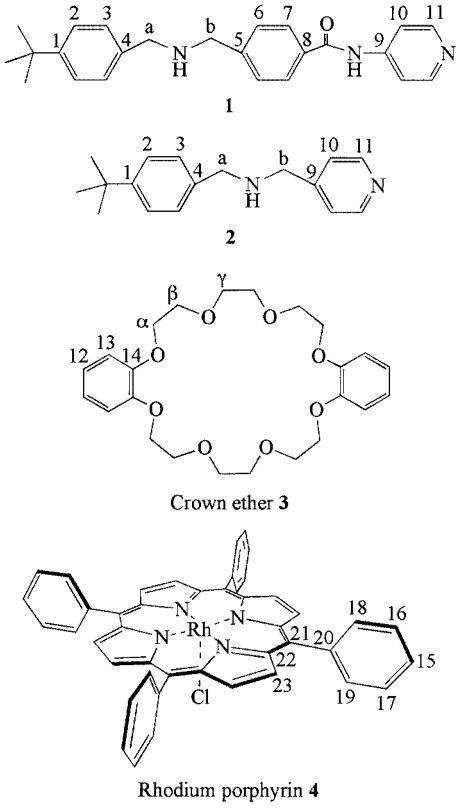

Figure 1. Chemical structures of the basic components and the labeling scheme for the NMR spectra assignment

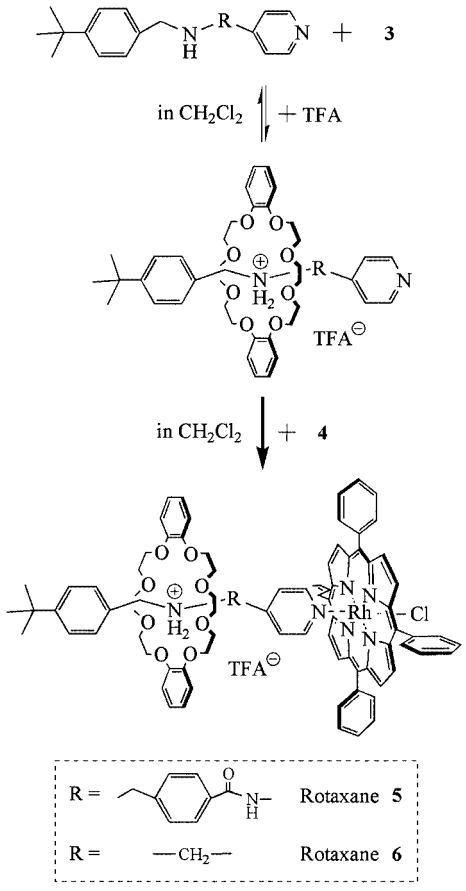

Figure 2. A schematic preparation scheme of the porphyrin-stoppered rotaxane; in the first step, inclusion complexation is a reversible process; in the second step, the coordination bond between the pyridine moiety of the thread molecule and rhodium(III) porphyrin chloride is extremely stable, so this capping reaction can be treated as an irreversible process at room temperature; the rotaxanes with thread molecules **1** and **2** are numbered **5** and **6**, respectively

ture providing much useful information on the molecular structure of the rotaxane.

In this study, 5,10,15,20-tetraphenylporphyrin rhodium chloride (rhodium porphyrin **4**, Figure 1) was used for end-capping. Here we describe the characterization of two tetraphenylporphyrin-stoppered rotaxanes (rotaxane **5** and **6**, Figure 2) with two kinds of thread molecules of different molecular lengths (**1** and **2**, Figure 1). We characterized the molecular structure of porphyrin-stoppered rotaxane in solution and in the solid state by NMR and X-ray crystallography.

Results and Discussion

Porphyrin-Stoppered Rotaxane 5

Figure 3 (a) shows a ^1H NMR spectrum of a $CDCl_3$ solution containing equimolar amounts of **1**, crown ether **3**, and trifluoroacetic acid (TFA). As would be expected, inclusion complexation was found to occur between the trifluoroacetate salt of **1** (**1**H-CF_3COO) and crown ether **3**.[8] Two sets of signals attributable to complexed (relatively larger signals labeled by numbers and letters)[9] and uncomplexed (free **1**H-CF_3COO and crown ether **3**, relatively small signals with *) species appeared separately, indicating that the exchange rate between complexed and uncomplexed species is slow on the NMR timescale. By use of rotating frame Overhauser effect spectroscopy (ROESY) we confirmed the through-space interactions between the methylene protons of crown ether **3** (α, β, and γ) and the aromatic protons of **1**H-CF_3COO (3 and 6) (data not shown). From the integrals of the signals in the ^1H NMR spectrum, the association constant was calculated to be ca. 3000 $L \cdot mol^{-1}$ [10] by the single-point method.[12]

Figure 3 (b) shows a ^1H NMR spectrum of the rotaxane **5** in $CDCl_3$. We found that all of the protons belonging to **1**H-CF_3COO and crown ether **3** show upfield shifts in comparison with those in Figure 3 (a). In particular, aromatic protons 11, situated in the position nearest to the terminal porphyrin, were drastically shifted upfield, because of the shielding effect of the diamagnetic current of the porphyrin ring.[7] The intensity of the shielding effect increased exponentially with decreasing distance from the porphyrin plane (Figure 4). This chemical shift change served as a good probe for estimation of the location of the mechanically interlocked crown ether **3**. The chemical shift changes for the methylene protons of crown ether **3** (α, β, and γ) are found to be approximately 0.21 ppm, indicating that crown ether **3** locates around the secondary ammonium ion group of the thread molecule.

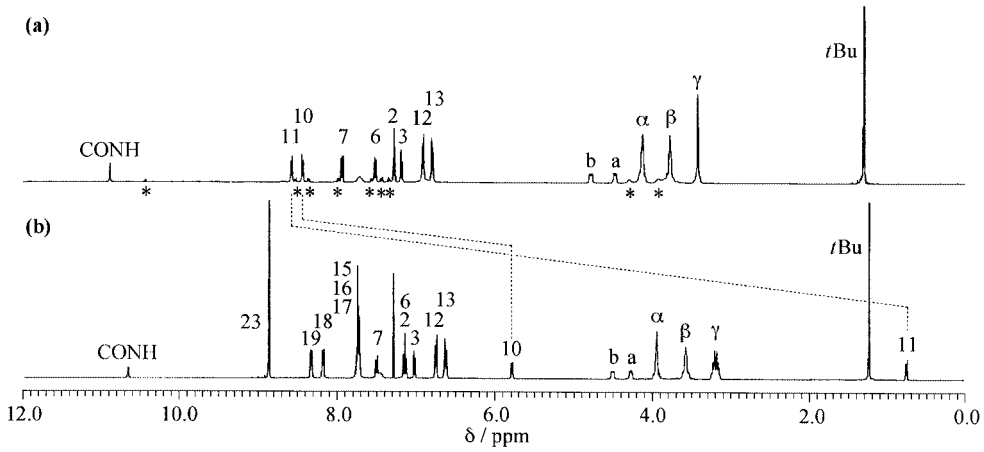

Figure 3. ^{1}H NMR spectra of: (a) mixture containing equimolar amount of **1**, crown ether **3**, and TFA, and (b) porphyrin-stoppered rotaxane **5** (400 MHz, $CDCl_3$, 293 K); the peaks labeled * in spectrum (a) are assignable to the protons of the uncomplexed species (free **1**H-CF_3COO and crown ether **3**)

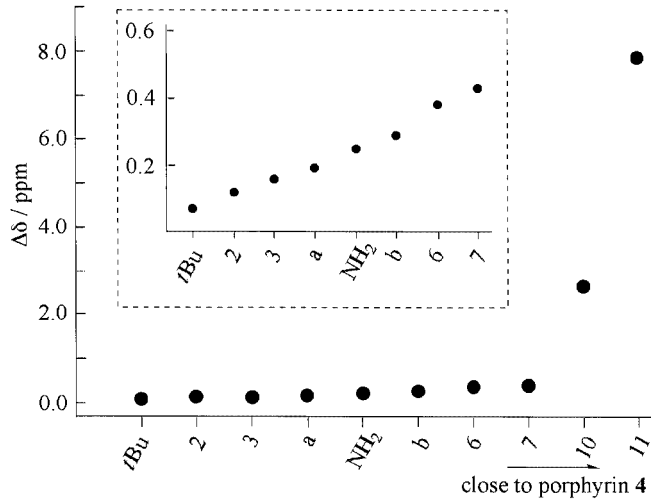

Figure 4. Shielding effect of the porphyrin on the thread molecule (**1**H-CF_3COO); $\Delta\delta = \delta_{complex} - \delta_{rotaxane}$; the chemical shifts of the thread molecule were shifted upfield by the shielding effect of the terminal rhodium porphyrin **4**; the intensity of the shielding effect clearly depends on the distance from the porphyrin plane

As for the phenyl protons of rhodium porphyrin **4**, the *ortho* protons (18 and 19) clearly gave different chemical shifts, whereas the *meta* and *para* protons' signals (15, 16, and 17) overlapped.[13] It is considered that the shielding effect of the coordinated pyridine moiety affects the chemical shift of the *ortho* protons 18.

Porphyrin-Stoppered Rotaxane 6

Figure 5 (a) shows a ^{1}H NMR spectrum of a $CDCl_3$ solution containing equimolar amounts of the trifluoroacetate salt of **2** (**2**H-CF_3COO) and crown ether **3**. Only one set of signals appeared, implying that the exchange rate between complexed and uncomplexed species is fast on the NMR timescale. The proton signals assignable to *t*Bu and to the aromatic protons 2 and 3 showed sharp peaks, whereas the other signals were broadened. Table 1 shows the difference in the chemical shifts between **2**H-CF_3COO in Figure 5 (a) and free **2**H-CF_3COO. The large positive $\Delta\delta$ value and the significant broadening of the methylene protons b suggest hydrogen bond formation between the methylene protons b and the ether oxygen atoms of crown ether **3**. All $\Delta\delta$ values for the protons of **2**H-CF_3COO, except for the aromatic

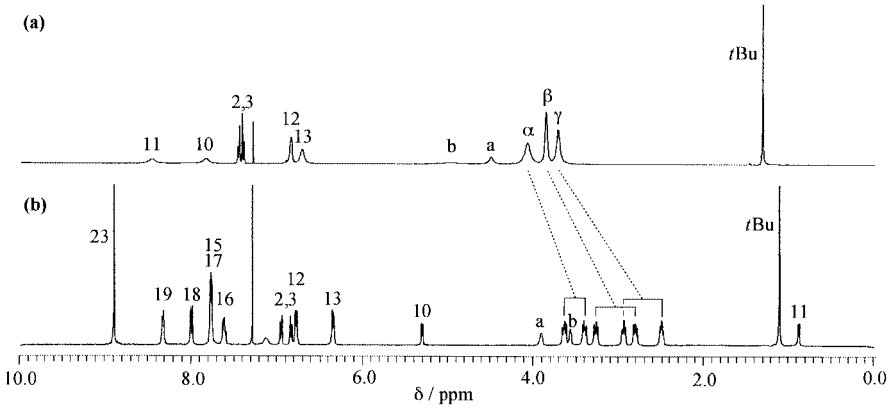

Figure 5. ^{1}H NMR spectra of: (a) mixture containing equimolar amount of **2**H-CF_3COO and crown ether **3**, and (b) porphyrin-stoppered rotaxane **6** (400 MHz, $CDCl_3$, 293 K); the complexed and uncomplexed species could not be distinguished

protons 11, were positive, due to the deshielding effect of the catechol ring in complexed crown ether **3**. The negative $\Delta\delta$ value for the aromatic protons 11**,** which implies that the aromatic protons 11 experience a shielding effect, suggests that the two catechol rings of crown ether **3** should sandwich the pyridine moiety of **2**H-CF_3COO to produce a π-π stacking interaction. These attractive interactions may reduce the local mobility around a, b, 10, 11 and crown ether **3**, resulting in the broadening of these peaks.

Table 1. Chemical shift changes between **2**H-CF_3COO in Figure 5 (a) and free **2**H-CF_3COO (400 MHz in $CDCl_3$ at 293 K)

Position	δ_{free}[a]/ppm	$\delta_{Fig5(a)}$[b]/ppm	$\Delta\delta$[c]/ppm
*t*Bu	1.21	1.30	+0.09
2	7.38	7.45	+0.07
3	7.27	7.40	+0.13
a	3.84	4.48	+0.64
b	3.95	4.98	+1.03
10	7.44	7.80	+0.36
11	8.59	8.45	−0.14

[a] Chemical shift of free species (**2**H-CF_3COO). [b] Chemical shift of **2**H-CF_3COO in Figure 5 (a). [c] $\delta_{Fig5(a)} - \delta_{free}$.

Figure 5 (b) shows a ^{1}H NMR spectrum of the rotaxane **6** in $CDCl_3$. We found that the methylene protons of crown ether **3** show six separated peaks, because of the magnetically unsymmetrical environments of these protons in the rotaxane. As shown in Figure 6, one side of the macrocycle faces towards the *t*Bu group (far side from the porphyrin plane) and another side towards the porphyrin stopper (near side to the porphyrin plane). The methylene protons located at the near- and far-side faces were labeled as (α-*n*, β-*n*, and γ-*n*) and as (α-*f*, β-*f*, and γ-*f*), respectively. Heteronuclear multiple quantum correlation spectroscopy (HMQC) and ROESY measurements enabled us to assign these protons. HMQC measurement clarified that the methylene protons (α-*n,* α-*f*), (β-*n,* β-*f*) and (γ-*n,* γ-*f*) belong to the carbons C_α, C_β and C_γ, respectively (data not shown). The ROESY spectrum showed cross-peaks between the methylene protons (α-*n*, β-*n*, and γ-*n*) and the aromatic protons 10, and not the aromatic protons 3. On the other hand, the methylene protons (α-*f*, β-*f*, and γ-*f*) showed the cross-peaks with the aromatic protons 3, and not the aromatic protons 10 (Figure 7). These results indicated that the protons (α-*n*, β-*n*, and γ-*n*) and the protons (α-*f*, β-*f*, and γ-*f*) are on the near- and the far-side faces of the macrocycle, respectively. Although the rotaxane **5** also has an unsymmetrical structure, no significant peak separation in the ^{1}H NMR spectrum took place for the methylene protons of crown ether **3** [Figure 3 (b)]. This is attributable to the feature of the shielding effect profile. As shown in Figure 4, the shielding effect of the porphyrin ring is very sensitive to changes in distance in the region near to the porphyrin plane. The effect, however, decreases drastically with increasing distance. The environmental differences between each face of the macrocycle in the rotaxane **5** would thus be too small to distinguish.

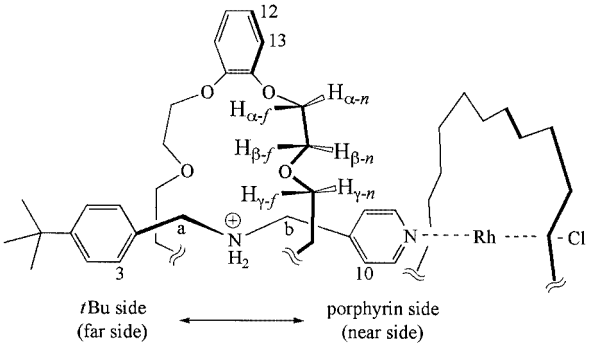

Figure 6. Schematic illustration of the rotaxane **6** indicating the unsymmetrical environments of the methylene protons of crown ether **3**; the protons located on the near- and far-side faces from the porphyrin are labeled $H_{\alpha\text{-, }\beta\text{-, }\gamma\text{-}n}$ and $H_{\alpha\text{-, }\beta\text{-, }\gamma\text{-}f}$, respectively

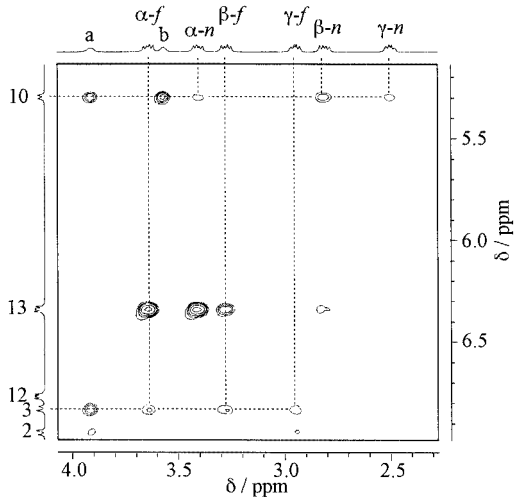

Figure 7. Partial ROESY spectrum for the rotaxane **6** (400 MHz, $CDCl_3$, 293 K); the protons of 10 and 3 show correlations to the methylene protons of crown ether located on the near- and far-side faces relative to the terminal porphyrin, respectively

Clearly, not only the *ortho* phenyl protons of rhodium porphyrin **4** (18 and 19), but also the *meta* phenyl protons (16 and 17), gave the different chemical shifts in the rotaxane **6**.[13] ROESY spectroscopy showed cross-peaks between the catechol protons of crown ether **3** (13) and the phenyl protons of rhodium porphyrin **4** (16 and 18) (data not shown). Crown ether **3** is located so close to the terminal rhodium porphyrin that the shielding effect of the catechol ring should affect the phenyl protons of 16 and 18. These NMR analyses supported the stable interlocked structure of the rotaxane **6** in $CDCl_3$.

The three-dimensional structure of the rotaxane **6** in the solid state was clarified by X-ray crystallography (Figure 8).[15] The secondary ammonium ion is encircled by crown ether **3** and trifluoroacetate counter-ion (Figure 9). TFA interacts with the secondary ammonium ion both electrostatically and through hydrogen bonding [(a) in Figure 9]. The hydrogen bond interactions (NH···O) contribute to stabilization of the supramolecular structure of **2** and crown ether **3** [(H···O) distances for (b) and (c), 2.15 and

2.03Å, respectively]. Although the hydrogen bonds between the methylene hydrogen atoms of **2** and the ether oxygen atoms [(H···O) distances for (d) and (e): 2.51 and 2.60 Å respectively] seem to be weak, they could also support the conformation of the complex. The β-hydrogen atoms of the pyridine moiety were found to be close to the ether oxygen atoms [(H···O) distances for (f), (g), and (h): 2.53, 2.43 and 2.36 Å, respectively]. Since these values are significantly smaller than that estimated from van der Waals radii (2.8 Å),[16] the molecular interactions (f), (g), and (h) are also to be regarded as hydrogen bonds. Because of the electron-donating feature of the axially coordinated pyridine to the rhodium(III) porphyrin,[17] the β-hydrogen atoms of the pyridine moiety may easily participate in hydrogen bond interaction. Although π-π stacking interactions between aromatic groups of crown ether **3** and the secondary dibenzylammonium cation derivatives have been reported,[3,11] we could not detect any π-π stacking interaction for the rotaxane **6**.

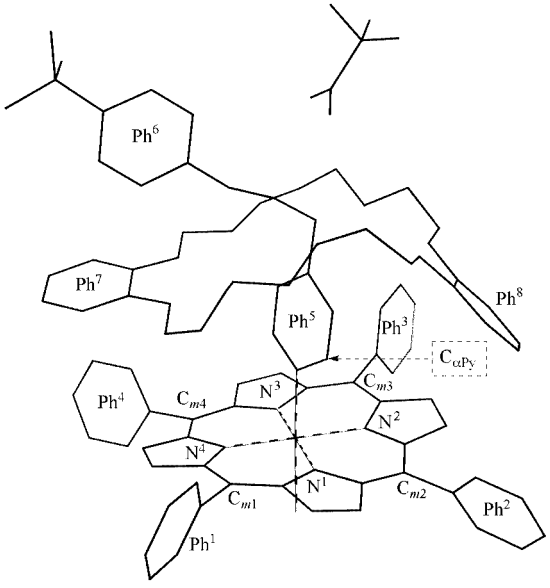

Figure 8. Molecular structure of the rotaxane **6** and labeling scheme for the phenyl groups ($Ph^1 - Ph^8$), *meso* C atoms, the nitrogen atoms of pyrrole groups ($N^1 - N^4$), and the carbon atom bearing the α-hydrogen atom of the pyridine moiety ($C_{\alpha Py}$); all of the hydrogen atoms and the solvent molecule are omitted for simplification

The rhodium atom has octahedral coordination (Figure 8). The equatorial $Rh-N_{pyrrole}$ (2.03Å) and the axial $Rh-N_{pyridine}$ (2.06Å) bond lengths are similar to the other coordination bonds in rhodium porphyrin complexes.[18] The axial Rh−Cl bond length (2.33Å) is also within the range usually observed in Rh^{III} complex.[19] The porphyrin core experiences significant distortion from planarity (Table 2). The *meso* C atoms of rhodium porphyrin **4** [$C_{m1}-C_{m4}$, Figure 8] are displaced alternately above and below the least-squares plane of the 20 carbon atom porphyrin core; this indicates that ruffling of the core is superimposed on a saddle deformation.[18] The distortion of the porphyrin core should be a result of unfavorable steric repulsive forces between $N_{pyrrole}$ and the α-hydrogen atoms of the pyridine moiety. In the case of the rotaxane **6**, the $N^1-Rh-N_{pyridine}-C_{\alpha Py}$ torsion angle is 30°, and the $C_{\alpha Py}H\cdots N^1$ distance is 2.53 Å. These values are significantly smaller[20] than those reported,[22] [e.g., 41° and 2.66 Å for pyridine-coordinated tetraphenylporphyrin rhodium(III) iodide[18]]. There seems to be a favorable interaction between the catechol rings and the phenyl groups of rhodium porphyrin **4** ($Ph^2\cdots Ph^8$ and $Ph^4\cdots Ph^7$). Presumably, the phenyl groups of rhodium porphyrin **4** are likely to interact with the catechol rings through aromatic CH-π interaction.[23] The small $N^1-Rh-N_{pyridine}-C_{\alpha Py}$ torsion angle may arise from this interaction. The dihedral angles of the phenyl group of rhodium porphyrin **4** with respect to the least-squares plane of the porphyrin core range from 75° to 115° (Table 3); these values are within the usual values for the tetraphenylporphyrin derivatives.[18,22]

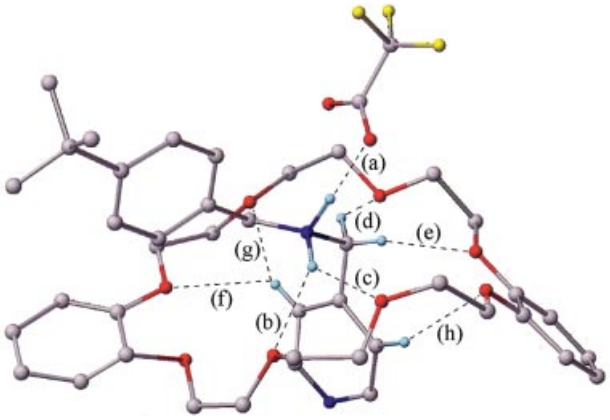

Figure 9. Partial molecular structure of the rotaxane **6**; rhodium porphyrin **4**, the solvent and the hydrogen atoms not participating in the molecular interaction are omitted for simplification; hydrogen bonding distances and angles [(X···O), (H···O) distances [Å], X−H···O angles [°]] (a) 2.78, 1.70, 168; (b) 2.98, 2.15, 135; (c) 2.86, 2.03, 135; (d) 3.23, 2.51, 138; (e) 3.18, 2.60, 123; (f) 3.21, 2.53, 133; (g) 3.25, 2.43, 151; (h) 3.18, 2.36, 152.

Table 2. Displacement of carbon and nitrogen atoms from the 20-carbon-atom least-squares plane of the porphyrin core

Atom label	Distance/Å	Atom label	Distance/Å
C_{m1}	0.200	N^1	0.013
C_{m2}	−0.195	N^2	−0.035
C_{m3}	0.237	N^3	−0.070
C_{m4}	−0.279	N^4	0.035

Figure 10 shows the molecular packing of the rotaxanes **6**. We confirmed the absence of characteristic interactions such as π-π or CH-π interactions between the rotaxanes **6** in the crystal.

Conclusion

The characterization of tetraphenylporphyrin-stoppered rotaxanes in $CDCl_3$ solution was carried out by NMR. From ^1H NMR measurements for the rotaxane **5**, we confirmed that the shielding effects of the terminal porphyrin

Table 3. Dihedral angles (°) between aromatic planes

	Ph^2	Ph^3	Ph^4	Ph^5	Ph^6	Ph^7	Ph^8	porphyrin[a]
Ph^1	96.75	20.12	91.07	113.94	46.39	106.45	68.59	107.26
Ph^2		90.94	38.57	19.33	50.48	66.31	105.31	75.52
Ph^3			98.51	110.13	45.55	86.47	51.63	87.17
Ph^4				36.25	54.29	104.53	137.84	113.58
Ph^5					67.74	71.32	118.77	79.63
Ph^6						88.23	87.24	95.28
Ph^7							52.16	9.26
Ph^8								46.84

[a] 20-carbon-atom least-squares plane of the porphyrin core.

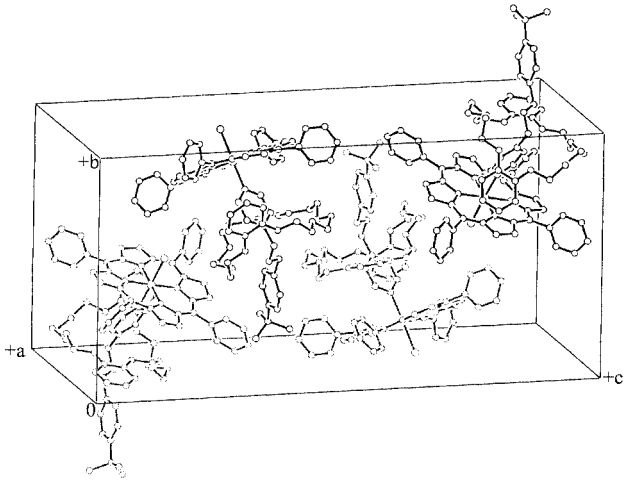

Figure 10. Molecular packing of four rotaxanes **6** in a unit cell [a = 13.900(2), b = 17.247(4), c = 34.923(5)Å, β = 93.46(2)°]; the hydrogen atoms, the trifluoroacetate, and the solvent molecules are omitted for simplification

molecule considerably affect the protons of **1**H-CF_3COO and crown ether. Crown ether **3** was shown to be around the secondary ammonium cation group of **1**H-CF_3COO by use of the shielding intensity as a probe. In the case of the rotaxane **6**, the methylene protons on crown ether **3** afforded six separated proton signals, due to the strong shielding effect of the terminal rhodium porphyrin **4**. Crown ether **3** proved to be close to the terminal rhodium porphyrin **4**, as shown by the ROESY spectrum and by the shielding effect of the catechol ring on the phenyl groups of rhodium porphyrin **4**. X-ray crystallography revealed many hydrogen bonds between **2**H-CF_3COO and crown ether **3**. In particular, the hydrogen bond formation between the β-hydrogen atoms of the pyridine moiety and the ether oxygen atoms is characteristic of the porphyrin-stoppered rotaxane **6**. In the solid state, four pyrrole groups of rhodium porphyrin **4** are exposed to magnetically nonequivalent environments by crown ether **3**. Namely, the pyrrole groups containing N^2 and N^4 are close to the catechol rings of crown ether **3**, and the other pyrrole groups containing N^1 and N^3 are more distant. In solution, however, we observed no remarkable peak splitting of the pyrrole protons and carbons in NMR spectra at 293 K. This is presumably due to fast conformation change on the NMR timescale and/or small chemical shift difference between two states.

Experimental Section

General: Tetracarbonyl-di-μ-chlorodirhodium(I) ($[Rh(CO)_2Cl]_2$) and crown ether **3** were purchased from Sigma−Aldrich Co. TFA was purchased from Wako Pure Chemical Industries. 5,10,15,20-Tetraphenylporphyrin was purchased from Tokyo Chemical Industry Co. Solvents were purchased from commercial sources. All chemical reagents were used without further purification. The amino derivative (**1**)[6] and trifluoroacetate salt of **2** (**2**-CF_3COO)[24] were prepared by the method described elsewhere. Column chromatography was carried out on Wakogel® C-200, Wakogel® C-400HG (Wako Pure Chemical Industries) and Sephadex™ LH-20 (Amersham Biosciences). ^1H and ^{13}C NMR spectra were recorded on a Bruker AVANCE 400 spectrometer (400 and 100 MHz for ^1H and ^{13}C NMR, respectively) with use of residual solvent as the internal standard. All chemical shifts are quoted on the δ scale. All 2D NMR experiments were recorded with 1 K data points and 256 time increments in phase-sensitive mode and processed in a 1 K × 1 K matrix. The ROESY experiment was performed with a spin lock mixing time of 200ms, and processed with a forward linear prediction in the F1 dimension. $^1H-^{13}C$ correlation by heteronuclear zero and double quantum coherence (HMQC and HMBC) experiments were performed with gradient pulses. In HMBC experiment, data was processed with low-pass J-filter to suppress one-bond correlations.

Amine 1:[6] White solid (Yield: 50%). ^1H NMR (400 MHz, $CDCl_3$, 20 °C): δ = 1.34 (s, 9 H, *t*Bu), 3.79 (s, 2 H, C_aH_2), 3.86 (s, 2 H, C_bH_2), 7.28 (d, $^3J_{H,H}$ = 8.3 Hz, 2 H, C^3H), 7.39 (d, $^3J_{H,H}$ = 8.3 Hz, 2 H, C^2H), 7.46 (d, $^3J_{H,H}$ = 8.2 Hz, 2 H, C^6H), 7.65 (dd, 2 H, $C^{10}H$), 7.84 (d, $^3J_{H,H}$ = 8.2 Hz, 2 H, C^7H), 8.50 (dd, 2 H, $C^{11}H$), 8.71 (s, 1 H, CONH) ppm. ^{13}C NMR (100 MHz, $CDCl_3$, 20 °C): δ = 31.8 (*t*Bu), 34.9 (*t*Bu), 53.1 (C_a), 53.3 (C_b), 114.4 (C^{10}), 125.9 (C^2), 127.9 (C^7), 128.3 (C^3), 128.9 (C^6), 133.1 (C^8), 137.2 (C^4), 145.7 (C^5), 145.9 (C^9), 150.6 (C^1), 151.1 (C^{11}), 166.8 (C=O).

Trifluoroacetate Salt of 2 (2H-CF_3COO):[24] White powder (Yield: 70%). ^1H NMR (400 MHz, $CDCl_3$, 20 °C): δ = 1.21 (s, 9 H, *t*Bu), 3.84 (s, 2 H, C_aH_2), 3.95 (s, 2 H, C_bH_2), 7.27 (d, $^3J_{H,H}$ = 8.4 Hz, 2 H, C^3H), 7.38 (d, $^3J_{H,H}$ = 8.4 Hz, 2 H, C^2H), 7.44 (d, $^3J_{H,H}$ = 6.2 Hz, 2 H, $C^{10}H$), 8.59 (d, $^3J_{H,H}$ = 6.2 Hz, 2 H, $C^{11}H$) ppm. ^{13}C NMR (100 MHz, $CDCl_3$, 20 °C): δ = 31.5 (*t*Bu), 35.1 (*t*Bu), 49.1 (C_b), 50.9 (C_a), 125.4 (C^{10}), 126.7 (C^2), 127.1 (C^4), 130.3 (C^3), 142.4 (C^9), 148.9 (C^{11}), 153.7 (C^1).

Rhodium Porphyrin 4: Tetraphenylporphyrin (0.45 g) and $[Rh(CO)_2Cl]_2$ (0.50 g) were dissolved in dry toluene (300 mL). The mixture was stirred for 6 h at room temperature. The solution was concentrated to 100 mL by evaporation, and silica gel (100 g) was added. The solvent was completely evaporated, and the residue was then heated at 60 °C for 1.5 h under normal pressure (the color of the silica gel changed from brown to red). The product was eluted from the silica gel (CH_2Cl_2/MeOH, 9:1). Chromatographic purification [Wakogel® C-400HG (silica gel), solvent: CH_2Cl_2/toluene/MeOH, 65:32:3] followed by recrystallization from CH_2Cl_2/hexane afforded the rhodium porphyrin **4** as a purple solid (Yield: 0.25 g, 45%); R_f = 0.27 (CH_2Cl_2). ^1H NMR (400 MHz, CD_2Cl_2, 20 °C): δ = 7.81−7.91 (m, 12 H, $C^{16}H$, $C^{17}H$, $C^{15}H$), 8.28 (d, $^3J_{H,H}$ = 7.8 Hz, 8 H, $C^{18}H$, $C^{19}H$), 9.01 (s, 8 H, $C^{23}H$) ppm. ^{13}C NMR (100 MHz, $CDCl_3$, 20 °C): δ = 122.4 (C^{21}), 127.2, 127.5 (C^{16}, C^{17}),

128.4 (C^{15}), 133.1 (C^{23}), 134.6, 135.0 (C^{18}, C^{19}), 142.4 (C^{20}), 143.6 (C^{22}), 158.0 (CO_2) ppm. MS (MALDI): m/z = 716 $[M - Cl]^+$. $C_{44}H_{28}ClN_4Rh\ CO_2$ (795.1): calcd. C 67.98, H 3.55, N 7.05; found C 67.80, H 3.78, N 6.95.

General Procedure for Rotaxane Preparation: Compound **1** (24 mg, 6.4×10^{-5} mol) and crown ether **3** (88 mg, 2.0×10^{-4} mol) were dissolved in CH_2Cl_2 (5 mL). TFA (10μL) was added to the solution, and the solvent was evaporated. The residue was dissolved in a small amount of CH_2Cl_2 and added to a CH_2Cl_2 solution (2.5 mL) containing rhodium porphyrin **4** (49 mg, 6.5×10^{-5} mol). The product was purified by chromatography (Wakogel® C-400HG: gradient elution from ethyl acetate to MeOH, Sephadex™ LH-20: MeOH).

Rotaxane 5: Purple solid (Yield: 80%); R_f = 0.32 (CH_2Cl_2/MeOH, 19:1). ^{1}H NMR (400 MHz, $CDCl_3$, 20 °C): δ = 0.75 (d, $^3J_{H,H}$ = 7.2 Hz, 2 H, $C^{11}H$), 1.23 (s, 9 H, *t*Bu), 3.18 (m, 8 H, $C_\gamma H$), 3.57 (m, 8 H, $C_\beta H$), 3.94 (m, 8 H, $C_\alpha H$), 4.27 (m, 2 H, C_aH_2), 4.51 (m, 2 H, C_bH_2), 5.77 (d, $^3J_{H,H}$ = 7.2 Hz, 2 H, $C^{10}H$), 6.62 (m, 4 H, $C^{13}H$), 6.74 (m, 4 H, $C^{12}H$), 7.03 (d, $^3J_{H,H}$ = 8.2 Hz, 2 H, C_3H), 7.13 (d, $^3J_{H,H}$ = 8.0 Hz, 2 H, C^6H), 7.15 (d, $^3J_{H,H}$ = 8.2 Hz, 2 H, C^2H), 7.46 (br., 2 H, NH_2), 7.50 (d, $^3J_{H,H}$ = 8.0 Hz, 2 H, C^7H), 7.68−7.78 (m, 12 H, $C^{15}H$, $C^{16}H$, $C^{17}H$), 8.17 (d, $^3J_{H,H}$ = 7.6 Hz, 4 H, $C^{18}H$), 8.32 (d, $^3J_{H,H}$ = 6.8 Hz, 4 H, $C^{19}H$), 8.87 (s, 8 H, $C^{23}H$), 10.65 (s, NHCO) ppm. ^{13}C NMR (100 MHz, $CDCl_3$, 20 °C): δ = 31.6 (*t*Bu), 35.1 (*t*Bu), 52.4 (C_b), 52.7 (C_a), 68.6 (C_α), 70.4 (C_β), 70.8 (C_γ), 113.1 (C^{10}), 113.2 (C^{13}), 121.5 (C^{21}), 122.3 (C^{12}), 125.9 (C^2), 126.8 (C^{17}), 127.0 (C^{16}), 127.8 (C^{15}), 128.8 (C^4), 128.9 (C^7), 129.1 (C^3), 129.3 (C^6), 132.8 (C^{23}), 135.0 (C^{19}), 135.0 (C^8), 135.2 (C^{18}), 135.3 (C^5), 142.7 (C^{22}), 142.8 (C^{20}), 146.0 (C^9), 146.1 (C^{11}), 147.6 (C^{14}), 153.0 (C^1), 166.7 (C=O) ppm. $C_{94}H_{88}ClF_3N_7O_{11}Rh{\cdot}H_2O$ (1705.1): calcd. C 66.21, H 5.32, N 5.75; found C 66.40, H 5.19, N 5.35.

Rotaxane 6: Purple solid (Yield: 75%); R_f = 0.20 (CH_2Cl_2/MeOH 19:1). ^{1}H NMR (400 MHz, $CDCl_3$, 20 °C): δ = 0.88 (d, $^3J_{H,H}$ = 6.4 Hz, 2 H, $C^{11}H$), 1.11 (s, 9 H, *t*Bu), 2.51 (m, 4 H, $H_{\gamma-n}$), 2.82 (m, 4 H, $H_{\beta-n}$), 2.95 (m, 4 H, $H_{\gamma-f}$), 3.27 (m, 4 H, $H_{\beta-f}$), 3.41 (m, 4 H, $H_{\alpha-n}$), 3.57 (br., 2 H, C_bH_2), 3.63 (m, 4 H, $H_{\alpha-f}$), 3.91 (br., 2 H, C_aH_2), 5.29 (d, $^3J_{H,H}$ = 6.4 Hz, 2 H, $C^{10}H$), 6.34 (m, 4 H, $C^{13}H$), 6.77 (m, 4 H, $C^{12}H$), 6.82 (d, $^3J_{H,H}$ = 8.2 Hz, 2 H, C^3H), 6.94 (d, $^3J_{H,H}$ = 8.2 Hz, 2 H, C^2H), 7.12 (br., 2 H, NH_2), 7.62 (m, 4 H, $C^{16}H$), 7.77 (m, 8 H, C_{15} H, $C^{17}H$), 7.99 (d, $^3J_{H,H}$ = 7.4 Hz, 4 H, $C^{18}H$), 8.33 (d, $^3J_{H,H}$ = 6.0 Hz, 4 H, $C^{19}H$), 8.90 (s, 4 H, $C^{23}H$) ppm. ^{13}C NMR (100 MHz, $CDCl_3$, 20 °C): δ = 31.5 (*t*Bu), 34.9 (*t*Bu), 48.0 (C_b), 51.6 (C_a), 68.0 (C_α), 70.0 (C_β), 70.5 (C_γ), 112.6 (C^{13}), 121.7 (C^{21}), 122.1 (C^{12}), 123.1 (C^{10}), 125.7 (C^2), 126.8 (C^{16}), 127.5 (C^{17}), 128.2 (C^{15}), 128.3 (C^4), 129.3 (C^3), 132.9 (C^{23}), 134.5 (C^{18}), 135.3 (C^{19}), 141.8 (C^9), 142.3 (C^{20}), 142.8 (C^{22}), 145.6 (C^{11}), 147.0 (C^{14}), 152.6 (C^1) ppm. $C_{87}H_{83}ClF_3N_6O_{10}Rh{\cdot}H_2O$ (1586.0): calcd. C 65.88, H 5.40, N 5.30; found C 65.83, H 5.19, N 5.06.

X-ray Crystallography

Crystal Data for Rotaxane 6: $[C_{85}H_{83}ClN_6O_8Rh][C_2F_3O_2]{\cdot}[C_4H_8O_2]$, M_r = 1656.11, monoclinic, space group $P2_1/c$ (no. 14), a = 13.900(2), b = 17.247(4), c = 34.923(5) Å, β = 93.46(2)°, V = 8356(2) Å^3, Z = 4, $\rho_{calcd.}$ = 1.316 g cm^{-3}, μ(Mo-K_α) = 3.07 cm^{-1}, F(000) = 3456.00, T = 203 K; clear prismatic crystal, 0.10 × 0.20 × 0.15 mm, Rigaku AFC7R diffractometer, graphite monochromated Mo-K_α radiation, ω scans, 19108 independent reflections (total: 20557). The structure was solved by direct methods (SIR92) and expanded by Fourier techniques. The atoms of the solvated molecule (ethyl acetate) were found to be disordered. The non-hydrogen atoms, except for the solvated molecule, were refined anisotropically, while those of the solvated molecule were fixed after refinement for a few cycles isotropically. The hydrogen atoms were included but not refined. The hydrogen atoms of the solvated molecule were omitted. The final cycle of full-matrix, least-squares refinement on F^2 was based on all independent reflections (2θ < 55.02°) and 948 variable parameters, and converged (largest parameter shift was 0.06 times its esd) with unweighted and weighted agreement factors. R_1 = 0.063 [$I > 2.0\sigma(I)$], R = 0.165, R_ω = 0.182, goodness of fit = 1.19. The maximum and minimum peaks on the final difference Fourier map corresponded to 1.85 (near the solvated molecule) and −1.14 e$^-$Å^{-3}, respectively. All calculations were performed with the teXsan crystallographic software (Molecular Structure Corporation).

CCDC-204886 contains the supplementary crystallographic data for the rotaxane **6**. These data can be obtained free of charge via www.ccdc.cam.ac.uk/conts/retrieving.html (or from the Cambridge Crystallographic Data Center, 12 Union Road, Cambridge CB2 1EZ, UK; Fax: (internat.) +44-1223-336-033; or E-mail: deposit@ccdc.cam.ac.uk).

Acknowledgments

This study was supported by an Industrial Technology Research Grant Program from the New Energy and Industrial Technology Development Organization (NEDO) of Japan.

[1] C. J. Pedersen, *J. Am. Chem. Soc.* **1967**, *89*, 7017 −7036.
[2] [2a] J. S. Bradshaw, R. M. Izatt, A. V. Bordunov, C. Y. Zhu, J. K. Hathaway in *Comprehensive Suparamolecular Chemistry, Vol. 1* (Eds.: J. L. Atwood, J. E. D. Davis, D. D. MacNicol, F. Vögtle, G. W. Gokel), Pergamon, Oxford, **1996**, pp. 35 −95. [2b] R. M. Izatt, K. Pawluk, J. S. Bradshaw, R. L. Bruening, *Chem. Rev.* **1995**, *95*, 2529 −2586.
[3] For some recent examples: [3a] S.-H. Chiu, S. J. Rowan, S. J. Cantrill, J. F. Stoddart, A. J. P. White, D. J. Williams, *Chem. Commun.* **2002**, 2948−2949. [3b] N. Watanabe, T. Yagi, N. Kihara, T. Takata, *Chem. Commun.* **2002**, 2720−2721. [3c] S. J. Cantrill, A. R. Pease, J. F. Stoddart, *J. Chem. Soc., Dalton Trans.* **2000**, 3715 −3734. [3d] S. J. Cantrill, D. A. Fulton, A. M. Heiss, A. R. Peace, J. F. Stoddart, A. J. P. White, D. J. Williams, *Chem. Eur. J.* **2000**, *6*, 2274−2287.
[4] [4a] A. M. Elizarov, S. H. Chiu, J. F. Stoddart, *J. Org. Chem.* **2002**, *67*, 9175−918. [4b] C. P. Collier, G. Mattersteig, E. W. Wong, Y. Luo, K. Beverly, J. Sampaio, F. M. Raymo, J. F. Stoddart, J. R. Heath, *Science* **2000**, *289*, 1172−1175. [4c] V. Bermudez, N. Capron, T. Gase, F. G. Gatti, F. Kajzar, D. A. Leigh, F. Zerbetto, S. W. Zhang, *Nature* **2000**, *406*, 608−611.
[5] [5a] K. Chichak, M. C. Walsh, N. R. Branda, *Chem. Commun.* **2000**, 847−848. [5b] M. J. Gunter, N. Bampos, K. D. Johnstone, J. K. M. Sanders, *New J. Chem.* **2001**, *25*, 166 −173.
[6] M. Asakawa, T. Ikeda, N. Yui, T. Shimizu, *Chem. Lett.* **2002**, 174−175.
[7] H. Ogoshi, J. Setsume, T. Omura, Z. Yoshida, *J. Am. Chem. Soc.* **1975**, *97*, 6461−6466.
[8] The trifluoroacetate salt of **1** (**1**H-CF_3COO) could be obtained from the equimolar mixture of **1** and TFA in $CHCl_3$ as a white precipitate. Since **1**H-CF_3COO is not soluble in CH_2Cl_2 or $CHCl_3$, we were not able to obtain NMR spectroscopic data for **1**H-CF_3COO. In spite of the poor solubility of **1**H-CF_3COO, the inclusion complex consisting of **1**H-CF_3COO and crown ether **3** could be prepared by addition of TFA to a mixture of **1** and crown ether **3**.

[9] The chemical shifts of the complexed species of **1**H-CF_3COO and crown ether **3**: ^{1}H NMR (400 MHz, $CDCl_3$): δ = 1.30 (s, *t*Bu), 3.43 (br., $C_\gamma H_2$), 3.78 (br., $C_\beta H_2$), 4.13 (br., $C_\alpha H_2$), 4.47 (m, $C_a H_2$), 4.80 (m, $C_b H_2$), 6.79 (m, $C^{13}H$), 6.91 (m, $C^{12}H$), 7.18 (d, $^3J_{H,H}$ = 8.3 Hz, C^3H), 7.27 (d, $^3J_{H,H}$ = 8.3 Hz, C^2H), 7.51 (d, $^3J_{H,H}$ = 8.2 Hz, C^6H), 7.93 (d, $^3J_{H,H}$ = 8.2 Hz, C^7H), 8.43 (d, $^3J_{H,H}$ = 7.4 Hz, $C^{10}H$), 8.58 (d, $^3J_{H,H}$ = 7.4 Hz, $C^{11}H$), 10.89 (s, CONH).

[10] The association constant: K_a = [inclusion complex]/[**1**H-CF_3COO][**3**]. Concentration: 1.2 × 10^{-2} mol·L^{-1}, Temperature: 293 K. The association constant of **1**H-CF_3COO with crown ether **3** is much smaller than that between the dibenzylammonium cation and crown ether **3** in $CDCl_3$.[11a] The association constants strongly depend on the chemical structure of the thread molecule.[11b,11c] One of them[11c] is much smaller than our reported value.

[11] [11a] P. R. Ashton, E. J. T. Chrystal, P. T. Glink, S. Menzer, C. Schiavo, N. Spencer, J. F. Stoddart, P. A. Tasker, A. J. P. White, D. J. Williams, *Chem. Eur. J.* **1996**, *2*, 709−728. [11b] P. R. Ashton, P. T. Glink, J. F. Stoddart, P. A. Tasker, A. J. P. White, D. J. Williams, *Chem. Eur. J.* **1996**, *2*, 729−736. [11c] T. Takata, H. Kawasaki, S. Asai, N. Kihara, Y. Furusho, *Chem. Lett.* **1999**, 111−112.

[12] S. J. Cantrill, M. C. T. Fyfe, F. M. Raymo, J. F. Stoddart, in *NMR in supramolecular Chemistry* (Eds.: M. Pons), Kluwer Academic Publishers, Dordrecht, **1999**, pp.1−18.

[13] The rotation of the phenyl rings with regard to the porphyrin core around ambient temperature can be slow on the NMR timescale.[14] In the case of rhodium porphyrin **4** (no ligand molecule), the *ortho* protons showed only one signal in ^{1}H NMR spectrum. However, ^{13}C NMR afforded five peaks corresponding to *ortho* (C^{18} and C^{19}), *meta* (C^{16} and C^{17}), and *para* (C^{15}) phenyl carbons independently (see Exp. Sect.). As for the ^{13}C NMR of the rotaxane, five phenyl carbon peaks were shown in similar manner with rhodium porphyrin **4**. The assignment of the protons was confirmed by HMQC measurements.

[14] C. J. Medforth, in *The Porphyrin Handbook, Vol. 5* (Eds.: K. M. Kadish, K. M. Smith, R. Guilard), Academic Press, San Diego, **2000**, pp.1−80.

[15] The single crystals of the rotaxane **6** were obtained by the vapor-diffusion procedure [sample solution: ethyl acetate/CH_2Cl_2, 3:1, reservoir solution: diethyl ether]. We found that the crystal contains the rotaxane **6** and the solvent (ethyl acetate). No substantial interaction took place between the rotaxane **6** and ethyl acetate. The disorder of three fluorine atoms and the ethyl acetate caused the relatively large *R* values (R_1 = 0.063, R = 0.182, and R_w = *0.165)*.

[16] L. Pauling, in *The Nature of the Chemical Bonds*, Cornell Univ. Press, **1960**, pp.260, Table 7−20.

[17] Y. H. Liu, J. E. Anderson, K. M. Kadish, *Inorg. Chem.* **1988**, *27*, 2320−2325.

[18] G. B. Jameson, J. P. Collman, R. Boulatov, *Acta Crystallogr., Sect. C* **2001**, *57*, 406−408.

[19] [19a] K. J. Bradd, B. T. Heaton, C. Jacob, J. T. Sampanthar, A. Steiner, *J. Chem. Soc., Dalton Trans.* **1999**, 1109−1112. [19b] D. C. Thackray, S. Ariel, T. W. Leung, K. Menon, B. R. James, J. Trotter, *Can. J. Chem.* **1986**, *64*, 2440−2446.

[20] The unfavorable steric interaction due to the smaller $N^1-Rh-N_{pyridine}-C_{\alpha Py}$ torsion angle may be not so serious. The energy difference between $N^1-M-N_{pyridine}-C_{\alpha Py}$ torsion angle of 0° and 45° was calculated to be 1.7 kcal mol^{-1} on the rigid rotor model.[21]

[21] R. J. Abraham, I. Marsden, *Tetrahedron* **1992**, *48*, 7489−7504.

[22] [22a] N. Li, V. Petricek, P. Coppens, *Acta Crystallogr., Sect. C* **1985**, *41*, 902−905. [22b] T. Sakurai, K. Yamamoto, *Acta Crystallogr., Sect. B* **1975**, *31*, 2514−2517.

[23] The distances between the aromatic rings were not close enough to support aromatic CH-π interaction.

[24] M. Asakawa, T. Shimizu, in preparation.

Received May 14, 2003

